Synergistic Effect of a Novel Charring Agent and Ammonium Polyphosphate on the Flame Retardancy of Acrylonitrile Butadiene Styrene

Wang Jun, Jiangsong Yi, Xu-Fu Cai

Department of Polymer Science and Materials, State Key Laboratory of Polymer Materials Engineering, Sichuan University, Chengdu, China 610065

Received 30 May 2010; accepted 1 August 2010
DOI 10.1002/app.33115
Published online 8 November 2010 in Wiley Online Library (wileyonlinelibrary.com).

ABSTRACT: A novel charring agent, poly(*p*-propane terephthalamide) (PPTA), was synthesized with terephthaloyl chloride and 1,2-propanediamine through solution polycondensation at a low temperature. PPTA was used together with ammonium polyphosphate (APP) to prepare a novel intumescent flame retardant (IFR) for an acrylonitrile butadiene styrene (ABS) resin. The flammability and thermal stability of the IFR–ABS composites were investigated with limiting oxygen index, UL 94 vertical burning, and thermogravimetric analysis tests. The results showed that the IFR system had excellent flame retardancy and antidripping properties for ABS. The thermogravimetric curves suggested that there was a distinct synergistic effect of PPTA and APP, and this effect greatly promoted the char formation of the IFR–ABS composites and hence improved the flame retardancy. Additionally, the structure and morphology of char residues were studied with Fourier transform infrared and scanning electron microscopy.
© 2010 Wiley Periodicals, Inc. J Appl Polym Sci 120: 968–973, 2011

Key words: flame retardance; synthesis; thermal properties

INTRODUCTION

Acrylonitrile butadiene styrene (ABS) is a widely used as a thermoplastic material because of its good mechanical properties, chemical resistance, and processing advantages.[1] However, its easy combustibility and melt dripping limit its applications, so it is necessary to construct a flame-retardant composition for ABS resins. Bromine-containing compounds, such as decabromodiphenyl oxide and tetrabromobisphenol A, are very effective and show a good property/price ratio for the flame retardancy of ABS resins.[2] However, the use of these halogen-containing flame retardants has been limited because they lead to environmental problems through the generation of great quantities of toxic and corrosive fumes during combustion. Accordingly, the development of nonhalogenated flame-retardant systems has become an attractive and emergent subject. Among nonhalogenated flame retardants, intumescent flame retardants (IFRs) with particular char-yielding properties have been widely used in various polymeric materials.[3–7]

One characteristic of IFR systems is their formation of insulative, foamed, carbonaceous chars.[8] It has been reported that the char acts as a barrier between the fire and the polymer and results in the extinction of combustion; therefore, the flame retardancy of the underlying polymer is improved. The carbonization agents commonly used in intumescent formulations are polyols such as pentaerythritol, mannitol, and sorbitol.[9,10] These additives are confronted with the problems of exudation and water solubility. Furthermore, they are not compatible with the polymeric matrix, and this weakens the mechanical properties of the materials.

Therefore, a lot of work has recently been done on applications of different kinds of carbonization agents.[11–20] Triazines and their derivatives are good charring agents. These agents have excellent charring effect because they contain abundant nitrogen and possess a structure of tertiary nitrogen.[11–14] Hu et al.[11] synthesized a derivative of triazines and used it as a charring agent with ammonium polyphosphate (APP) in polyethylene. When the charring agent (8 wt %) and APP (22 wt %) were incorporated into polyethylene, the limiting oxygen index (LOI) reached the maximum of 31.2, and class V0 in the UL 94 test was obtained. Li and Xu[12] also combined a novel triazine charring–foaming agent with APP and used them in polypropylene. The results indicated that polypropylene with a flame-retardant concentration of only 18 wt % could obtain a V0

Correspondence to: X.-F. Cai (caixf2004@sina.com).
Contract grant sponsor: National Natural Sciences Foundation of China; contract grant number: 50973066.

© 2010 Wiley Periodicals, Inc.

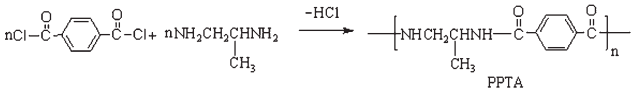

Scheme 1 Synthesis of PPTA.

rating with a high LOI value of 30.2. In addition, polyamides such as polyamide 6, polyamide 66, and polyamide 11 can be used as charring agents.[15–19] Polyamide 6 is a well-known char-forming polymer, and the interaction between the amide groups of polyamide 6 and an acid catalyst at a high temperature can form some crosslinking chemical structures, which strengthen the char layer. However, according to our previous study,[17] polyamide 6 has poor compatibility with ABS because of its relatively strong polarity. Therefore, in this work, we tried to prepare a high-melting-point, char-forming polymer that would not melt during the process and disperse in ABS as inorganic and rigid particles. On heating, this charring agent can react with an acid source rapidly to form a uniform and compact intumescent charred layer, which can protect the underlying materials from the action of heat and flame.

In this study, a novel charring agent, poly(*p*-propane terephthalamide) (PPTA), was synthesized (Scheme 1) and used together with APP to prepare a novel IFR for ABS. The synergistic effect of these two components on the flame retardancy and thermal properties of ABS was studied.

EXPERIMENTAL

Materials

An ABS copolymer (0215-A) was supplied by Jilin Petrochemical Co. (Jilin, China). APP was obtained from Zhejiang Longyou GD Chemical Industry Corp. (Longyou, China). Terephthaloyl chloride was supplied by Shanghai Xinliang Chemical Reagent Factory (Shanghai, China). 1,2-Propanediamine, calcium chloride ($CaCl_2$), and *N*-methyl-pyrrolidone were purchased from Kelong Chemical Reagent Corp. (Chengdu, China).

Synthesis of PPTA

A 150-mL, three-necked, round-bottom flask equipped with a stirrer was charged with 3.0 g of $CaCl_2$, 3.7 g (0.05 mol) of 1,2-propanediamine, and 100 mL of *N*-methyl-pyrrolidone. Then, the mixture was stirred, and when $CaCl_2$ was completely dissolved, the flask was cooled to 0–5°C. After that, 10.15 g (0.05 mol) of terephthaloyl chloride was added slowly to the flask within about 0.5 h, and the reaction temperature was kept at 0–10°C. Then, the flask was heated up to 45–50°C, and the reaction was completed after 2 h. Successively, the reaction mixture was cooled to room temperature, and then the mixture was poured into distilled water and filtered. The white solid was washed with water and dried *in vacuo* at 80°C to a constant weight.

Sample preparation

ABS resins with different APP and PPTA contents were mixed in a Haake plasticorder mixer at 220°C and 50 rpm for 7 min. The mixed samples were transferred to a mold and preheated at 220°C for 3 min; they were then pressed at 10 MP and successively cooled to room temperature while the pressure was maintained to obtain the composite sheets for further measurements. Before mixing, all the components were dried in a vacuum oven at 100°C for 12 h.

Characterization

IR spectroscopy was applied with a Nicolet IS10 Fourier transform infrared (FTIR) spectrometer (Nicolet Instrument Co., USA) with KBr pellets. ^{1}H-NMR (400 Hz) spectra were recorded on an FT-80A NMR (Varian Instrument Co., USA) instrument with CF_3COOD as the solvent. LOI data for all samples were obtained at room temperature with an oxygen index instrument (XYC-75) (Chende Jinjian Analysis Instrument Factory, China) produced by Chende Jinjian Analysis Instrument Factory according to the ASTM D 2863-77 standard. The dimensions of all samples were 130 × 6.5 × 3 mm^3. The vertical burning rates of all samples with dimensions of 125 × 12.5 × 3.2 mm^3 were measured on a CZF-2 instrument (Jiangning Analysis Instrument Factory, China) produced by Jiangning Analysis Instrument Factory according to the UL 94 test (ASTM D 635-77). The thermogravimetric analysis of the flame-retardant polymer was carried out on a WRT-2R thermal analyzer (Shanghai precision and Scientific Instrument, China) with a heating rate of 10°C/min from 50 to 700°C and with an atmospheric flow of 50 mL/min. The surface morphology of the char obtained after the LOI test was observed with a Hitachi X-650 scanning electron microscope (Hitachi, Japan). The FTIR spectra of the char residues were recorded on a Nicolet Magna-IR 560 spectrometer (Nicolet Instrument Co., USA) with a KBr plate technique.

RESULTS AND DISCUSSION

Characterization of PPTA

Figure 1 presents the FTIR spectrum of the synthesized PPTA. The absorption bands at 1541, 1497, and 3072 cm^{-1} correspond to vibrations of the benzene rings, and the peaks at 2976, 2932, and 2872 cm^{-1} have been assigned to —CH, —CH_2, and —CH_3. The absorptions at 1636 and 3293 cm^{-1} are associated with the stretching mode of C=O and N—H from the acrylamide group.

The ^{1}H-NMR spectrum of PPTA is shown in Figure 2. The peak at δ = 7.58 ppm has been assigned to aromatic protons. The peaks around δ = 3.61 ppm,

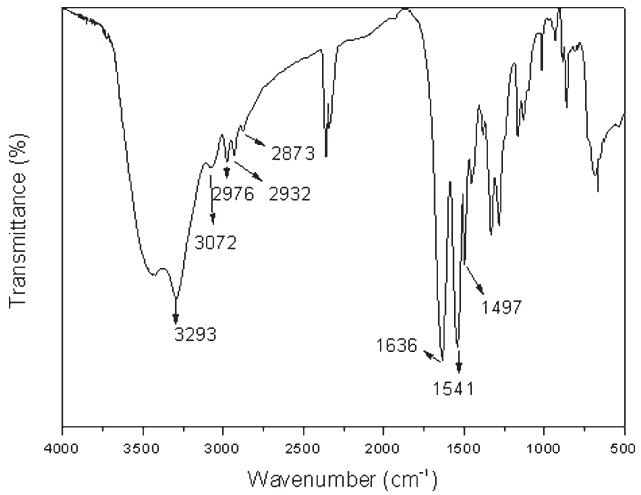

Figure 1 FTIR spectrum of PPTA.

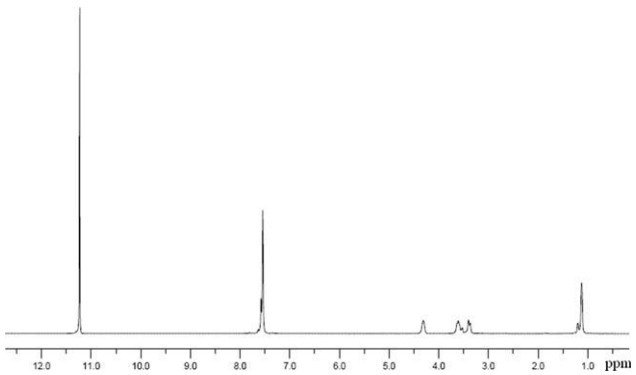

Figure 2 ^{1}H-NMR spectrum of PPTA.

$\delta = 3.40$ ppm, and $\delta = 1.12$ ppm correspond to the $-CH_2$ protons, $-CH$ protons, and $-CH_3$ protons, respectively. Additionally, the peaks at $\delta = 4.31$ ppm can probably be attributed to the N—H protons. All this information confirms that the target product was synthesized successfully.

Flammability

A series of flame retardants differing in their APP/PPTA ratio were manufactured, and they were compounded with ABS. Table I shows the LOI values and vertical burning rates for the IFR–ABS systems with a total loading of the APP and PPTA additives of 30 wt %. According to Table I, the LOI values of the ABS/APP system without PPTA and the ABS/PPTA system without APP were 25.2 and 24.6, respectively; both failed the UL 94 test. This demonstrated that APP and PPTA alone showed a low efficiency for ABS flame retardancy. However, when the mixture of APP and PPTA was incorporated into ABS, the LOI values of the IFR–ABS systems were dramatically increased, and LOI increased with the increasing addition of PPTA. When the weight ratio of PPTA to APP increased to 1:3, the LOI value of the IFR–ABS system reached a maximum of 31.6, and class V0 of UL 94 was passed. When the ratio of PPTA to APP continued to increase, the LOI value of the IFR–ABS systems decreased; that is, the LOI value decreased to 27.5 when the weight ratio of PPTA to APP was 1:1. These results proved that there was a distinct synergistic effect of PPTA and APP when they were applied to ABS.

Thermal analysis

In our investigation of the synergistic effect of PPTA and APP, thermogravimetric analysis was used to study their thermal degradation properties. Figure 3 shows the thermogravimetric and differential thermogravimetric curves of the APP, PPTA, and APP/PPTA (3:1) systems; relative data are listed in Tables II and III. PPTA was thermally stable below 260°C, its initial temperature was 292.5°C (based on 5% weight loss), and its thermal degradation occurred in two steps. The decomposition temperature in the first step ranged from 300 to 450°C, the second was between 550 and 650°C, and the main peak of thermal degradation was at 375.5°C; this was possibly due to the deacetylation reaction and the degradation of the carbon bond chain. When the temperature reached 700°C, PPTA decomposed completely, and no char residue existed. This demonstrated that PPTA itself had very poor charring ability. However,

TABLE I
Effect of PPTA on the Flame Retardancy of the IFR–ABS Systems

	Component (wt %)					
Sample	ABS	APP	PPTA	APP:PPTA	LOI (%)	UL 94
1	100	0	0	–	18.6	Failure
2	70	30	0	–	25.2	Failure
3	70	25	5	5:1	29.6	V1
4	70	24	6	4:1	30.7	V0
5	70	22.5	7.5	3:1	31.6	V0
6	70	20	10	2:1	28.7	V1
7	70	15	15	1:1	27.5	Failure
8	70	0	30	–	24.6	Failure

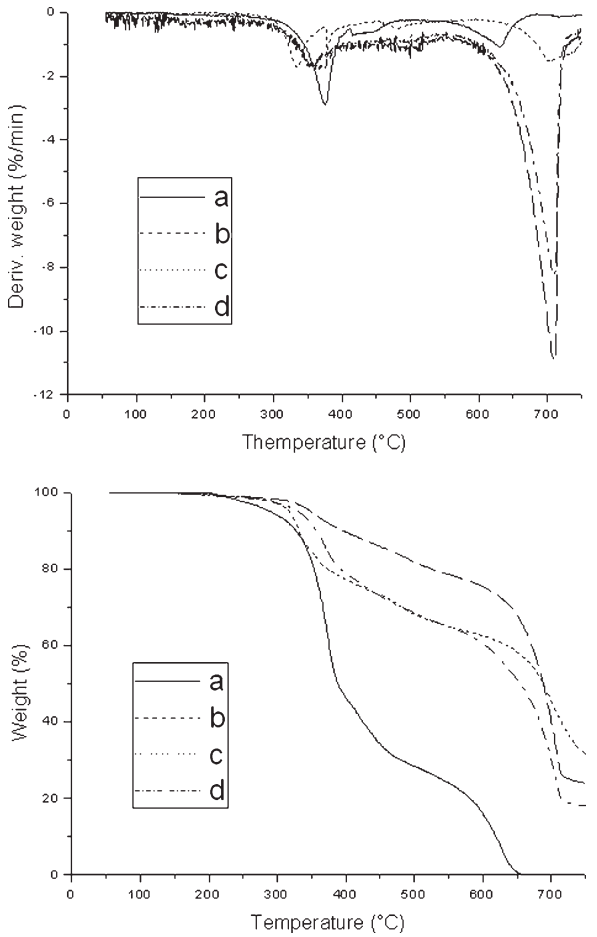

Figure 3 Thermogravimetric and differential thermogravimetric curves of the APP/PPTA systems: (a) PPTA, (b) APP, (c) APP/PPTA, and (d) APP/PPTA (calculation).

when PPTA was combined with APP, the decomposition course changed significantly, and a synergistic effect could be observed between them. Figure 3(d) shows the result calculated from Figure 3(a,b) on the basis of their percentages in the APP/PPTA (3:1) systems. Figure 3(c) presents the experimental results for the APP/PPTA (3:1) system. According to the experimental curve of the APP/PPTA system, the char residues at 500, 600, and 700°C were 68.2, 62.6, and 45.5 wt %, respectively, whereas the calculated values were 68.6, 60.5, and 30.0 wt %. These results indicated that when the temperature was above 600°C, the APP/PPTA system expressed higher thermal stability, and much more char residue was formed than was expected. Additionally, the differential thermogravimetric curves showed that the initial decomposition temperature and the temperature of the first decomposition peak of the APP/PPTA system were much lower than those calculated. Meanwhile, the decomposition speed at a higher temperature (ca. 700°C) was also much lower than that calculated. It could be speculated that APP catalyzed the decomposition of PPTA, reacted with PPTA at a relatively low temperature, and formed a crosslinking structure. Thus, the decomposition at higher temperatures was inhibited. Therefore, the char residues at high temperatures (>600°C) of the experimental curve were more than the calculated ones. These results indicated that the synergistic effect of PPTA and APP greatly strengthened the char-formation ability and thermal stability of the IFR system at high temperatures.

Figure 4 and Tables II and III provide thermal degradation data and curves for the ABS, IFR, and IFR–ABS (formulation 5) systems. The IFR components were APP (75 wt %) and PPTA (25 wt %). The thermal degradation of ABS showed two peaks at 438.8 and 575.2°C, and no char residue existed over 500°C. Figure 4(d) presents the calculated result based on Figure 4(a,b) and the IFR and ABS percentages in the IFR–ABS systems. A comparison of Figure 4(c,d) shows that the char residues of the experimental curve clearly increased at 500, 600, or 700°C. Meanwhile, we also found that IFR clearly led to a maximum peak of ABS decomposition at a higher temperature. The main decomposition peak of ABS took place at 438.8°C, whereas the main decomposition peak of ABS in the IFR–ABS system appeared at 465.4°C. This was probably attributable to the fact that the char layer formed by IFR prevented heat from transferring into the IFR–ABS system.

All these results proved that the synergistic effect of APP and PPTA could improve the char-formation ability of ABS and lead IFR–ABS to form more char. The char could protect the underlying polymer from flame, lower the heat-transfer coefficient between the

TABLE II
Thermal Degradation Data from Thermogravimetric Analysis

Sample	$T_{initial}$ (°C)	R_{1peak} (%/min)	T_{1peak} (°C)	R_{2peak} (%/min)	T_{2peak} (°C)
APP	350.3	1.83	360.4	10.93	710.6
PPTA	292.5	2.91	375.5	1.1	630.6
APP/PPTA (3:1)	318.1	1.45	331.9	1.38	697.6
ABS	392.0	21.98	438.8	1.69	575.2
ABS/APP/PPTA (70:22.5:7.5)	372.7	3.83	465.4	–	–

R_{1peak} = decomposition speed at the first decomposition peak; R_{2peak} = decomposition speed at the second decomposition peak; T_{1peak} = temperature of the first decomposition peak; T_{2peak} = temperature of the second decomposition peak; $T_{initial}$ = initial decomposition temperature (based on 5% weight loss).

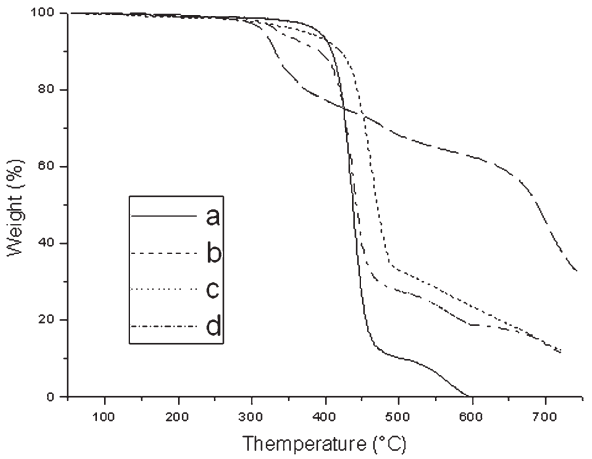

Figure 4 Thermogravimetric curves of the IFR–ABS systems: (a) ABS, (b) IFR, (c) IFR–ABS, and (d) IFR–ABS (calculation).

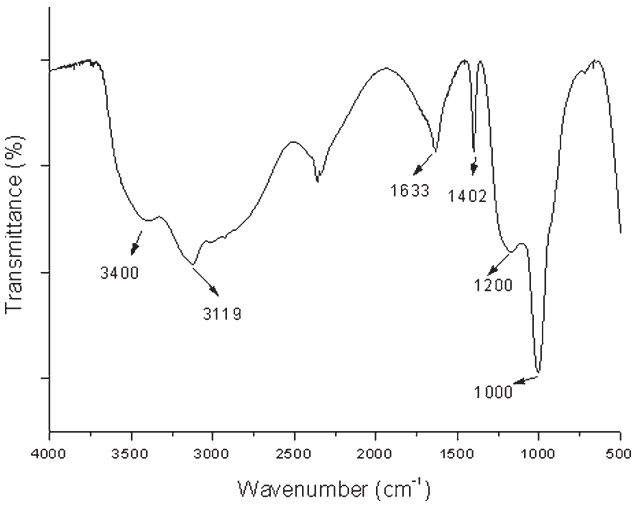

Figure 5 FTIR spectrum of the char from burning IFR–ABS (formation 5) in the LOI test.

flame and the polymeric material, and limit oxygen diffusion to the polymer; thus, the flame retardancy of ABS was enhanced.

Structural analysis of the combustion residue by FTIR

Figure 5 shows the FTIR spectrum of the residue obtained from LOI testing of IFR–ABS (formulation 5). The absorption band at 3406 cm^{-1} has been assigned to the stretching mode of —OH from the P—OH group, and the bands at 3119 and 1633 cm^{-1} correspond to the stretching mode of N—H in NH_4^+ and C=C stretching or polyaromatics, respectively.[20,21] The absorption band at 1200 cm^{-1} can be attributed to the P—O—C structure in the P—C complex, and the peak around 1000 cm^{-1} is due to the symmetric vibration of the P—O bond in the P—O—C group.[22] Meanwhile, the strong bands at the 2917-, 2843-, and 1402-cm^{-1} absorptions are due to the organic species in the residues.[23] Therefore, the FTIR spectrum confirms the existence of P—O—C chemical bonds in the char layers, and this indicates that a crosslinking reaction between PPTA and APP might have occurred. As mentioned previously, this crosslinking reaction would form some carbonaceous char residues with the matrix, and this could well protect the ABS matrix and exhibit antidripping effects.[13]

Morphology of the residue char

To explore how the structure of intumescent char determines the flame retardancy of ABS, we investigated the residues of char left after LOI testing for the char appearance by scanning electron microscopy (SEM). Figure 6 presents SEM micrographs of char residues of ABS/APP and IFR–ABS (formulation 5). According to Figure 6(a), for ABS with APP alone, there were many big holes due to insufficient char formation or less condensed char during the burning process. This poor char quality could not effectively protect the underlying ABS from degradation during combustion; therefore, in vertical burning tests, melt dripping was observed. However, the char surface of ABS with both APP and PPTA, illustrated in Figure 6(b), was compact, smooth, and tight. This structure of char for IFR–ABS composites could prevent heat transfer between the flame zone and the substrate and thus protect

TABLE III
Char Residues at 500, 600, and 700°C

	Char residue (%)					
	500°C		600°C		700°C	
Sample	Experimental	Calculated[a]	Experimental	Calculated[a]	Experimental	Calculated[a]
APP	82.0	–	75.5	–	40.0	–
PPTA	28.5	–	16.1	–	0	–
APP/PPTA (3:1)	68.2	68.5	62.6	60.5	45.5	30.0
ABS	10.2	–	0	–	0	–
ABS/APP/PPTA (70:22.5:7.5)	33.0	27.6	23.6	18.7	13.9	13.6

[a] Data for two components were added.

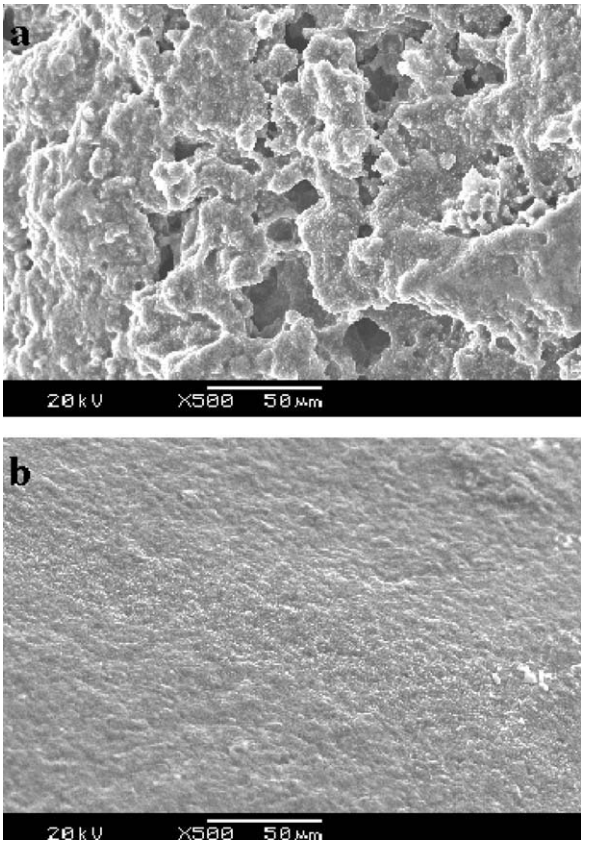

Figure 6 SEM photographs of residues of ABS/APP (formation 2) and IFR–ABS (formation 5).

the underlying materials from further burning and pyrolysis, so they had much higher LOI values. In addition, this char structure could offer a good shield to prevent melted ABS from dripping, and this was proved in vertical flammability tests.

CONCLUSIONS

A novel charring agent, PPTA, was synthesized successfully and was well characterized with ^{1}H-NMR and FTIR. The combination of PPTA and APP could form a very effective IFR, and the optimum weight ratio of APP to PPTA was 3:1. When the IFR concentration was 30 wt %, the LOI value of the IFR–ABS system was found to be 31.6, and a V0 rating was obtained. Thermogravimetric curves demonstrated that there was a synergistic effect between PPTA and APP, which could enhance the char-formation ability of the APP/PPTA system. The char residues of this system could reach 45.5 wt % at 700°C, whereas only 30.0 wt % was achieved according to calculations. This synergistic effect even enhanced the thermal stability of ABS and promoted ABS to form more char. The FTIR spectrum of char obtained from burning IFR–ABS (formulation 5) during LOI testing confirmed the existence of P—O—C chemical bonds in char layers, and this indicated that the crosslinking reaction between PPTA and APP had occurred. In SEM micrographs, a rich char layer could be observed, and this slowed heat and mass transfer between the gas and condensed phases.

References

1. Wang, S. F.; Hu, Y.; Song, L.; Wang, Z. Z.; Chen, Z. Y.; Fan, W. C. Polym Degrad Stab 2002, 77, 423.
2. Brebu, M.; Bhaskai, T.; Murai, K.; Muto, A.; Sakata, Y.; Uddin, M. A. Chemosphere 2004, 56, 433.
3. Chiu, S. H.; Wang, W. K. Polymer 1998, 39, 1951.
4. Le Bras, M.; Bugajny, M.; Lefebvre, J.; Bourbigot, S. Polym Int 2000, 49, 1115.
5. Zhu, W. M.; Weil, E. D.; Mukhopadhyay, S. J Appl Polym Sci 1996, 62, 2267.
6. Xie, R. C.; Qu, B. J. J Appl Polym Sci 2001, 80, 1181.
7. Horacek, H.; Pieh, S. Polym Int 2000, 49, 1106.
8. Gao, M.; Wu, W.; Yan, Y. J Therm Anal Calorim 2009, 95, 605.
9. Bras, M. L.; Bourbigot, S.; Delporte, C.; Siat, C.; Tallec, Y. L. Fire Mater 1996, 20, 191.
10. Bras, M. L.; Bourbigot, S.; Tallec, Y. L.; Laureyns, J. Polym Degrad Stab 1997, 56, 11.
11. Hu, X.; Li, Y.; Wang, Y. Z. Macromol Mater Eng 2004, 289, 208.
12. Li, B.; Xu, M. J. Polym Degrad Stab 2006, 91, 1380.
13. Ke, C. H.; Li, J.; Fang, K. Y.; Zhun, Q. L.; Yan, Q.; Wang, Y. Z. Polym Degrad Stab 2010, 95, 763.
14. Dai, J. F.; Li, B. J Appl Polym Sci 2010, 116, 2157.
15. Liu, Y.; Feng, Z. Q.; Wang, Q. Polym Compos 2010, 30, 221.
16. Almeras, X.; Dabrowski, F.; Bras, M. L.; Delobel, R.; Bourbigot, S.; Marosi, G.; Anna, P. Polym Degrad Stab 2002, 77, 315.
17. Lu, C. X.; Chen, T.; Cai, X. F. J Macromol Sci Phys 2009, 48, 651.
18. Ma, Z. L.; Zhang, W. Y.; Liu, X. Y. J Appl Polym Sci 2006, 101, 739.
19. Zhang, Y. X.; Liu, Y.; Wang, Q. J Appl Polym Sci 2009, 116, 45.
20. Peng, H. Q.; Zhou, Q.; Wang, D. Y.; Chen, L.; Wang, Y. Z. J Ind Eng Chem 2008, 14, 589.
21. Wang, D. Y.; Cai, X. X.; Qu, M. H.; Liu, Y.; Wang, J. S.; Wang, Y. Z. Polym Degrad Stab 2008, 93, 2186.
22. Mahapatra, S. S.; Karak, N. Polym Degrad Stab 2007, 92, 947.
23. Camino, G.; Sgobbi, R.; Zaopo, A.; Colombier, S.; Scelza, C. Fire Mater 2000, 24, 85.